Vancomycin: Conformational Consequences of the Sugar Substituent[||]

Simona Golic Grdadolnik,[†,§] Primoz Pristovšek,[†] and Dale F. Mierke*[,§,‡]

National Institute of Chemistry, Hajdrihova 19, 1001 Ljubljana, Slovenia, Gustaf H. Carlson School of Chemistry, Clark University, 950 Main Street, Worcester, Massachusetts 01610, and Department of Pharmacology and Molecular Toxicology, University of Massachusetts, Medical Center, 55 Lake Avenue North, Worcester, Massachusetts 01655

Received September 8, 1997

High-resolution, three-dimensional structures of vancomycin and aglyco-vancomycin in DMSO were determined by nuclear magnetic resonance, metric matrix distance geometry, and molecular dynamics calculations. Conformational flexibility fast on the NMR time scale was examined by ensemble-based calculations which apply the experimentally derived restraints as an ensemble average. Two families of conformations of vancomycin, differing in the positioning of the vancosamine substituent, were observed. In contrast, the aglyco-vancomycin adopts only one conformation in solution. The conformations of vancomycin and the aglyco-vancomycin differ in the alignment of the amide protons which participate in the hydrogen-bonding network with the cell-wall precursor and orientation of the aromatic rings relative to the backbone. Therefore, the high-resolution structural characterization provides insight into a possible role of glycosylation on the activity of this important family of antibiotics.

Introduction

Vancomycin (Figure 1) is the last effective drug against *Staphylococcus aureus* and other pathogens. It belongs to a family of glycopeptide antibiotics which all share similar, extended heptapeptide backbones with extensively cross-linked side chains and a variety of sugar substituents. A major advantage of vancomycin treatment has been the virtual absence of resistant strains. Thus, the recently discovered resistance to vancomycin in a number of *enterococci* strains[1,2] emerges as a crisis in antibiotic resistance[3] and is an object of intense study. The threat of other bacteria developing resistance has stimulated the design of new antibacterial agents.

Glycopeptide antibiotics inhibit the transglycosylation and transpeptidation steps in the synthesis of the cell-wall by noncovalent binding to the D-Ala-D-Ala terminus of the pentapeptide cell-wall precursor. Several high-field NMR studies of complexes involving various glycopetide antibiotics with cell-wall mimics such as Ac-L-Lys(Ac)-D-Ala-D-Ala and Ac-D-Ala-D-Ala have led to a model in which the complex is stabilized by a series of five hydrogen bonds between the peptide precursor and the antibiotic heptapeptide backbone.[4−7] Recently additional hydrogen-bonding interactions between the antibiotic and the rest of the pentapeptide cell-wall fragment were found in the complex of A82846B with the Ala-isoGlu-Lys-D-Ala-D-Ala pentapeptide.[8]

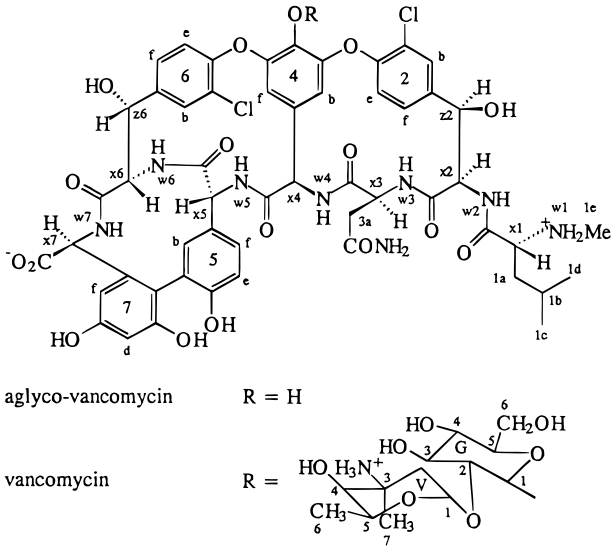

Figure 1. Primary structure of vancomycin illustrating the atom nomenclature used in this study.

In resistant bacteria the C-terminus of the cell-wall precursor is D-Ala-D-lactic acid, in which the terminal D-Ala is replaced with a lactic acid.[9] The 1000-fold reduced binding affinity of vancomycin for the modified precursor,[10] paralleling the decreased effectiveness of the antibiotic to the resistant bacteria,[9,11] can be attributed to elimination of one of the hydrogen bonds in the complex.[12]

An important physiological role has been attributed to the ability of the glycopeptide antibiotics to form homodimers in aqueous solution.[13−15] A cooperative effect between dimerization and ligand binding has been observed, and given the fact that the affinity of antibiotics to the cell-wall analogues correlates in many cases with in vitro antibiotic activity,[5] dimerization may have a positive effect on antibiotic activity.

The sugar substituents are believed to be responsible for a number of favorable interactions in the formation

[||] Abbreviations: NMR, nuclear magnetic resonance; COSY, correlated spectroscopy; DQF-COSY, double quantum-filtered COSY; TOCSY, total correlated spectroscopy; NOE, nuclear Overhauser effect; NOESY, NOE spectroscopy; HSQC, heteronuclear single-quantum correlation; DMSO, dimethyl sulfoxide; DG, distance geometry, MD, molecular dynamics; DDD, distance-driven dynamics; rmsd, root-mean-square deviation.

* Address for correspondence: Prof. D. F. Mierke, Department of Molecular Pharmacology, Box G-B4, Brown University, Providence, RI 02912. Tel: (401) 863-2139. Fax: (401) 863-1595. E-mail: Dale_Mierke@brown.edu.

[†] National Institute of Chemistry.

[§] Clark University.

[‡] University of Massachusetts.

S0022-2623(97)00597-9 CCC: $15.00
Published on Web 05/05/1998

of the dimer.[13,16] The ring 4 disaccharide promotes dimerization by a factor of ca. 100. The increase in the dimerization constant of A82846B by a factor of 250 with respect to vancomycin can be attributed to the presence of a ring 6 amino sugar in A82846B, the only difference between the two antibiotics.[13] Influence of the sugar substituents on the dimerization constants has led to a prediction that the antibiotic aglycons are less active. Indeed, experimental data indicate that the in vivo activity of aglyco-vancomycin is 5 times less than that of vancomycin.[17] However, the effect of the sugar substitution on the conformation of the heptapeptide backbone, which might influence the activity of the glycopeptide antibiotic, has not been examined.

Here we report the results of a structural comparison of vancomycin and its aglycon analogue. The aim is to obtain high-resolution, three-dimensional structures of both antibiotics and to examine the influence of the sugar substituent on conformation. This will provide structural insight into the observed differences in the activity of vancomycin and its aglycon analogue.

To concentrate on specific conformational differences in the absence of dimerization, our study was carried out in DMSO. It has been clearly illustrated that vancomycin dimerizes in water but not in DMSO. First the NMR-derived distance restraints were applied in metric matrix DG calculations[18] which provide a fast and complete search of conformational space. The conformational mobility fast on the NMR time scale was inspected by ensemble-based simulations.[19,20] The resulting structures were further refined by extensive molecular dynamics simulations carried out in explicit DMSO.[21] By the application of the force field used in the molecular dynamics simulations, important energetic features of the molecule are included and the DG structures, which are based only on molecular connectivity and experimental constraints, were verified. Moreover, the inclusion of explicit solvent molecules improves the energetic refinement given the large surface area of the molecules.

Results

The proton chemical shifts of vancomycin and aglyco-vancomycin were assigned following standard procedures using homonuclear DQF-COSY, TOCSY, and NOESY experiments in combination with $^{1}H-^{13}C$ HSQC experiments. The assignment is in agreement with previously published results for vancomycin.[22,23] The prochiral methylene protons of the asparagine residue were assigned by the method of floating chiralities[24] and by the simple method of testing both prochiral assignments during MD simulations. Allowing for the chiralities of the β-methylene protons of Asn-3 to float during the DG-based simulated annealing refinement resulted in a ratio of 3:1 with the low-field proton as *pro-R* (i.e., 25% of the resulting structures from the DG calculations had the high-field proton *pro-R*). To further examine this assignment, NOE-restrained MD simulations were carried out with both possible assignments. In accord with the DG results, the calculations with the high-field proton as *pro-R* resulted in distorted structures with amide bonds deviating strongly out of plane and with large NOE violations centered around residues 2, 3, and 4. The assignment of *pro-R* to the low-field proton did not produce such distortions.

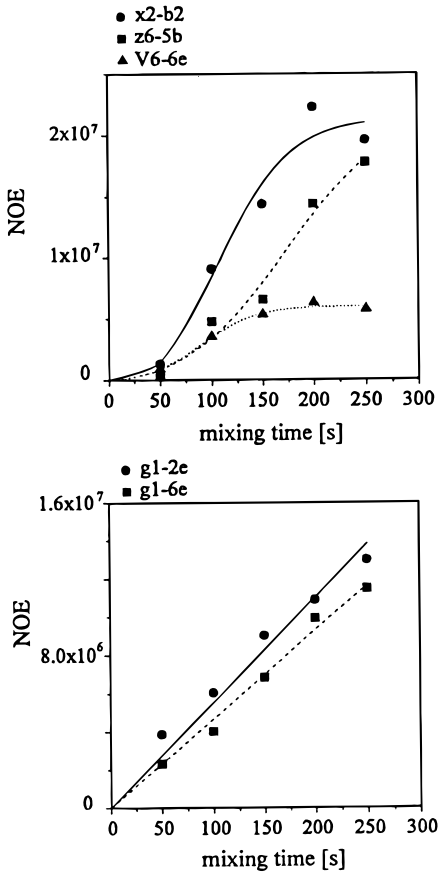

Figure 2. Selected buildup curves of the NOEs of vancomycin which are influenced by spin diffusion. The g1−2e and g1−6e NOEs, which are linear in the range from 0 to 250 ms, and therefore not affected by spin diffusion, are shown for comparison.

The proton−proton distances were calculated from NOESY spectra measured at 150 ms using the two-spin approximation and the integrated intensity of a geminal pair of protons assumed to have a distance of 1.78 Å. Both antibiotics are in the negative NOE regime when studied in DMSO at 298 K. In previous NMR studies of this class of compounds in DMSO, spin diffusion was assumed to have only a limited effect on the NOEs measured at 400 and 500 MHz.[7,25] In contrast, the NOESY spectra of vancomycin in DMSO measured at 600 MHz display significant spin-diffusion effects between z6−x5, z6−5b, 5b−4f, x5−x4, and 2b−x2 protons in both antibiotics and additionally between 6e−V6, V2−G3, and G4−V1 protons in vancomycin. These effects were identified by the examination of NOESY spectra collected at many different mixing times (50, 100, 150, 200, and 250 ms). Examples of the nonlinear behavior in the initial stage of the NOE buildup curve for these pairs of protons are given in Figure 2. The buildup curves of g1−2e and g1−6e NOEs, which are linear in the range from 0 to 250 ms, are shown for comparison. The NOEs between x5−x4, 5b−4f, V2−G3, and G4−V1 were not observed in the 50-ms NOESY and were of medium intensity in the 150-ms NOESY, and therefore they were not utilized in the structural refinement calculations discussed below. For the proton pairs z6−x5, z6−5b, 2b−x2, and 6e−V6 the distances calculated from the 50-ms NOESY (a mixing time in which the NOE buildup is still linear) were utilized.

Table 1. Distances (Å) Calculated from NOESY Spectra of Aglyco-vancomycin and Vancomycin

atoms		aglyco-vancomycin	vanco-mycin	atoms		aglyco-vancomycin	vanco-mycin
1e	2f	3.7	3.5	x6	6b	2.7	2.5
x2	hoz2	3.2	2.7	x6	w7	2.1	2.1
x2	w3	2.5	2.4	w6	hoz6	2.4	2.4
x2	z2	2.3	2.2	w6	6f	2.6	2.5
x2	2b	2.9	3.4	z6	hoz6	2.3	2.2
z2	2f	2.9	3.3	z6	w6	3.4	3.4
z2	hoz2	2.3	2.2	z6	6b	2.3	2.3
z2	2b	2.3	2.4	z6	6F	3.4	3.4
2e	4b	3.3	3.4	z6	w7	2.6	2.5
2f	hoz2	2.8	2.8	hoz6	6b	3.7	3.8
2f	w2	3.5	2.5	hoz6	6e	3.8	3.7
2f	$3a^S$	2.9	3.3	hoz6	6f	2.6	2.5
x3	w3	3.1	3.0	6b	w7	3.2	3.0
x3	$3a^R$	2.8	2.7	x7	w7	2.6	2.9
x3	$3a^S$	2.5	2.3	x7	7f	3.8	3.5
w3	$3a^R$	3.3	3.1	w7	7f	3.3	3.7
w3	$3a^S$	3.4	3.2	x2	2f	3.4	
w3	4b	3.7	3.5	z2	w3	4.0	
$3a^S$	3b1	2.6	2.6	hoz2	2b	3.5	
$3a^S$	3b2	3.4	3.4	2b	4b	4.4	
$3a^R$	3b1	2.6	2.7	$3a^S$	2e	3.3	
$3a^R$	3b2	3.4	3.5	2f	$3a^R$	2.8	
$3a^S$	4b	3.6	3.3	2f	4b	3.7	
x4	w4	3.3	3.0	$3a^S$	w4	2.6	
x4	w5	2.1	2.1	x4	5f	4.2	
x4	4f	3.0	2.8	x5	6f	4.2	
x4	4b	2.3	2.7	w5	w6	4.0	
4b	w4	2.6	2.4	5e	x7	4.0	
4f	w5	2.9	2.7	5f	x7	4.6	
4f	x5	2.8	2.8	x6	6f	3.6	
4f	6e	3.4	3.3	w6	w7	3.8	
4f	6b	3.5	4.0	w6	x7	4.5	
x5	w5	2.6	2.8	hoz6	w7	4.0	
x5	5b	2.1	2.0	x2	w2		3.2
X5	5F	3.6	3.7	2e	G1		3.2
X5	X6	1.8	1.8	2e	V6		3.8
X5	Z6	3.7	3.8	6e	G1		3.6
X5	W6	3.3	2.8	6e	V6		4.6
X5	6B	3.1	2.9	6e	V7		3.8
X5	W7	2.7	2.9	6b	V7		4.6
W5	5F	3.0	2.9	G1	V5		2.8
5B	Z6	4.0	3.7	G1	V7		3.8
5B	6B	3.6	3.4	G2	V1		2.1
5B	W7	2.2	2.2	G2	V5		2.7
5B	X6	2.1	2.2	G2	V6		3.8
X6	W6	2.8	2.9	G2	V7		4.1
X6	Z6	2.3	2.3	G3	V1		2.7
X6	HOZ6	3.5	3.9	G3	V7		4.4

Interestingly, each of the pairs of protons identified above to be involved in spin diffusion was found later (during the structural refinement discussed below) to have an intermediate proton spatially between them, ideal for indirect NOE enhancement. There are 64 common distance constraints between the antibiotics which were utilized in the structure refinement (Table 1). In addition 17 and 15 unique constraints were applied for aglyco-vancomycin and vancomycin, respectively (Table 1).

With the exception of a x2−w2 constraint, the vancomycin-unique constraints involve protons between the two saccharides and between the disaccharide unit and aromatic rings 2 and 6. Most of the aglyco-vancomycin-unique constraints are weak and do not influence the structural changes observed between vancomycin and aglyco-vancomycin (i.e., these NOEs are fulfilled, no violations greater than 0.3 Å, by the resulting structures of vancomycin). Exceptions are medium constraints 2f−$3a^R$ and 2e−$3a^S$ (Figure 3), which are violated in all

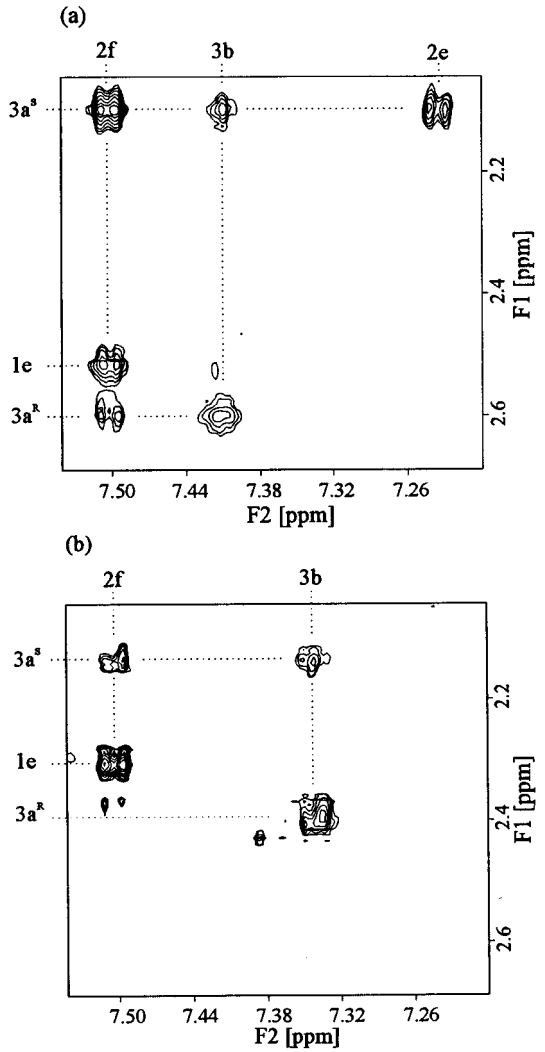

Figure 3. Expanded regions of NOESY spectra of aglyco-vancomycin (a) and vancomycin (b) showing the different NOE pattern of the methylene protons of residue 3.

vancomycin structures by more than 0.5 Å. These two constraints indicate a different alignment of the Asn-3 side chain in vancomycin and aglyco-vancomycin.

The DG calculations of aglyco-vancomycin resulted in 98 structures with an rmsd value of 0.9 Å for all heavy atoms and with an average NOE violation of 0.1 Å. Conformations are highly ordered in the constrained cyclic part of the molecule with a dihedral angle order parameter[26] greater than 0.9 (Figure 4), whereas the conformation of residue 1, which is outside the constrained ring system, is less ordered. Despite this appearance of order, there are 5 structures out of the 98 which have different orientations of the amide w3 proton, manifested by different ψ_2 and ϕ_3 dihedral angles as depicted in the Ramachandran map for residue 3 (Figure 5). The w3 proton is projecting toward the front of the binding pocket in the minor group of conformations (5 structures) and toward the rare side of the aglycon in the major group of conformations (93 structures). A representative structure from both of these groups was chosen and subjected to extensive NOE-restrained MD simulations. During the MD simulation beginning with the minor conformation, there is a transition to the major conformation with the amide proton projecting to the rare side of the aglycon. The

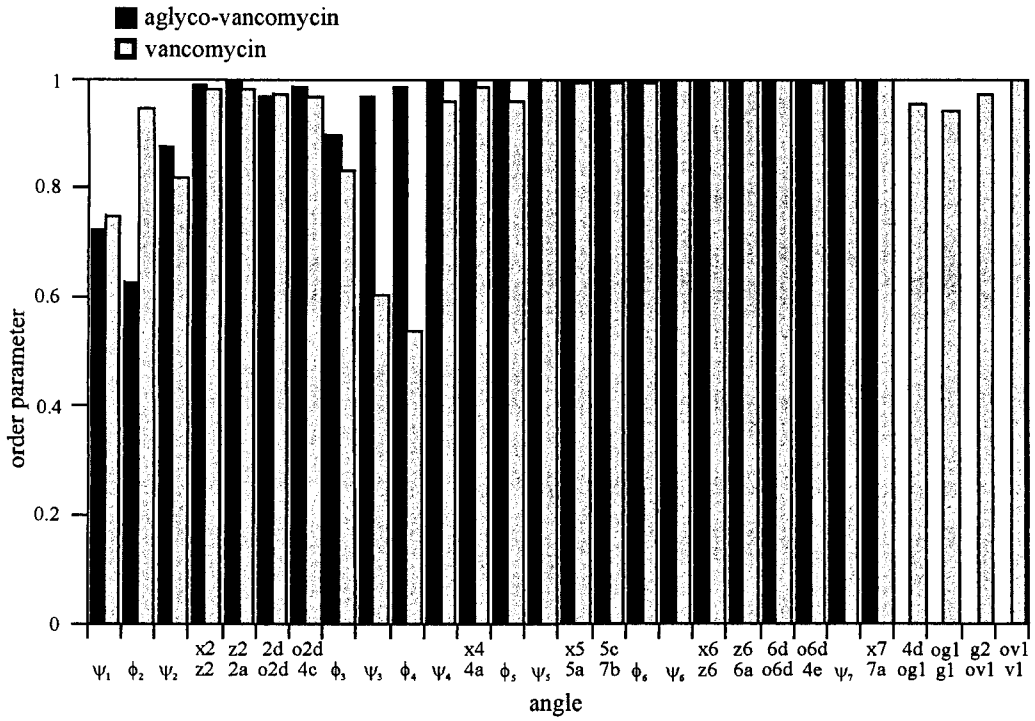

Figure 4. Dihedral angle order parameters calculated for the structures resulting from the DG calculations of aglyco-vancomycin and vancomycin.

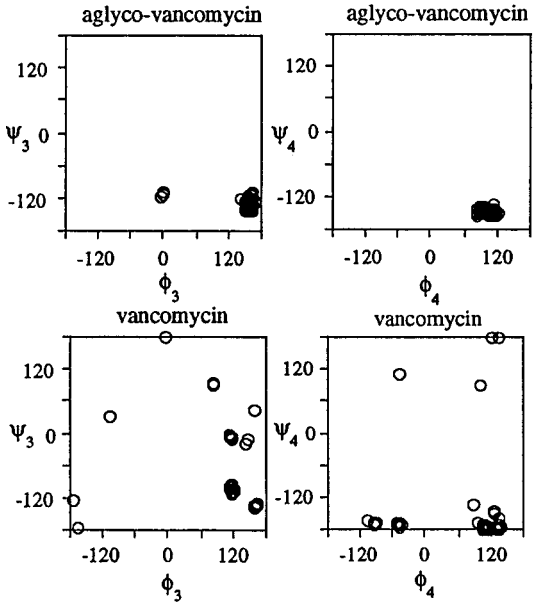

Figure 5. Ramachandran maps of the ϕ and ψ torsions of residues 3 and 4 of aglyco-vancomycin and vancomycin of the resulting structures from the DG calculations.

average dihedral angles from both simulations calculated from the last 100 ps of the simulation are almost identical and indicate that the rigid framework of the aglyco-vancomycin adopts one conformation in DMSO. The average NOE distance violation from the restrained simulation is 0.08 Å. Only one NOE violation larger than 0.4 Å is observed: 1e−2f with a value of 0.47 Å. This may be an indication that residue 1, which is not constrained in the cyclic part of the molecule, can adopt many conformations in DMSO, and therefore an ensemble-based simulation protocol[19] would be required.

In contrast to aglyco-vancomycin, the DG calculations of vancomycin show more conformational flexibility in the ring composed of residues 2, 3, and 4. The calculations resulted in 65 structures with an rmsd value of 1.1 Å for all heavy atoms and an average NOE violation of 0.16 Å. Noteworthy the ψ_3 and ϕ_4 dihedral angles have much lower-order parameters, and the Ramachandran plots of residues 3 and 4 illustrate the presence of several families (Figure 5). One of the families has the Asn side chain aligned on the rare side of the molecule. The other three families have the Asn side chain in front of the aglycon and differ in the orientation of the w3 and w4 amide protons. The remainder of the molecule comprising residues 5, 6, 7 and the two saccharides adopts one conformation and is highly structured, with high dihedral angle order parameters.

Even with different starting structures, the molecular dynamics simulations always resulted in violations of a NOE between 2e−G1, sometimes with violations as high as 2 Å. This is an indication that the experimental constraints between the disaccharide and the aromatic rings of the antibiotic aglycon cannot be satisfied by a single conformation. These observations are in agreement with the previously published model of two different conformations of vancomycin differing by a 180° rotation around the glucose 4 glycosidic linkage.[5] To address the problem of conformational mobility of the disaccharide substituent, ensemble calculations were performed. The starting ensemble was generated by copying the resulting 65 DG structures five times. Only the average of the members of the ensemble is required to satisfy the experimental constraints, and thus the fast conformational averaging which occurs in solution is properly described.[19,20] The resulting structures have two orientations of the sugar substituent differing by approximately 180° (Figure 6). One orientation, with the vancosamine on the rare side of the molecule, satisfies the 2e−G1 and 6e−V6 NOEs and is also in agreement with the observation of a weak NOE between

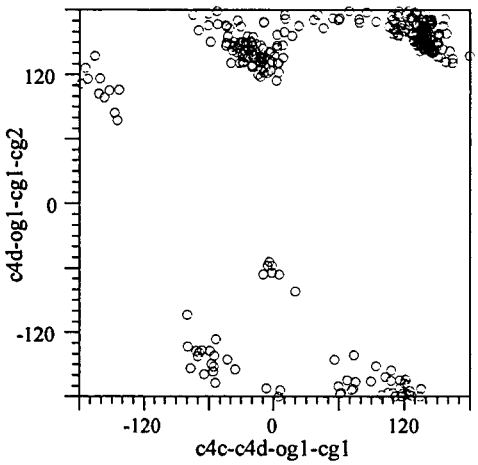

Figure 6. Ramachandran map of the c4c−c4d−og1−cg1 and c4d−og1−cg1−cg2 dihedral angles defining the orientation of the disaccharide substituent relative to the antibiotic aglycon, resulting from the ensemble-based DG calculations.

the 2e and V7 protons. In the second orientation, the V6 methyl group is aligned in front of the aglycon and V7 is above ring 6; this conformation fulfills the observation of the G1−6e, 6e−V7, and 6b−V7 NOEs. Therefore, assuming an ensemble of two conformational families, and that the experimental observations are averaged from this ensemble, the constraints are fulfilled. To further refine the ensemble-generated structures, extensive MD simulations with explicit solvent were carried out. Ensemble averaging of the experimental constraints was not utilized during the MD simulations. Instead, we carried out standard MD simulations with eight different starting structures, differing in the orientation of the sugar substituent and the ψ_3 and ϕ_4 dihedral angles as observed in the ensemble-based DG structures (Figure 5). Depending on the starting structure, a different set of NOEs between the disaccharide and aglycon was included in the simulations; i.e., only the NOEs which are consistent with the particular sugar orientation were included. The two simulations starting with the side chain of Asn aligned on the rare side of the molecule resulted in very high-energy structures with distortions (the amide bonds of residues 3 and 4 well-removed from planarity). Therefore, the inclusion of important energetic features (i.e., partial charges, Coulombic interactions, Lennard−Jones attractive forces) in the structure determination allows us to exclude this family of DG structures as possible conformations of vancomycin in DMSO; they will not be considered further. The other six simulations resulted in two families of structures differing by the positioning of the disaccharide (Figure 7). The average distance restraint violation from the simulations is between 0.09 and 0.1 Å; only one large NOE violation (x2−w3 violated by 0.6 Å) was observed in all of the simulations. This violation is discussed below.

Discussion

In Table 2 the average values for the dihedral angles, calculated over the last 100 ps of the MD production period of aglyco-vancomycin and vancomycin, are summarized. The different orientations of the disaccharide substituent with the V6 methyl group either in front or on the rare side of the molecule are denoted as positions 1 and 2, respectively. The largest deviations of the torsions from the average values during the MD production period are 10°.

There are several notable differences between the two conformational families of vancomycin and aglyco-vancomycin. These will be discussed in terms of the position of the sugar substituents, orientation of the aromatic rings relative to the antibiotic backbone, and alignment of the amide protons which participate in the hydrogen-bonding network of the antibiotic complex with the cell-wall precursor or form hydrogen bonds in the antibiotic homodimer.

The most obvious difference between the two families of vancomycin conformations is the position of the sugar substituent, which is rotated by approximately 200° about the glycosidic linkage of glucose ring 4 (Table 2). In one conformation, the V7 methyl group lies above ring 6 and the V6 methyl group in front of the glucose ring 4 glycosidic linkage (Figure 7A,C). A similar alignment of the vancosamine is observed in the crystal structure of CDP-I [27] and in the complex of the vancomycin with the tripeptide Ac-L-Lys(Ac)-D-Ala-D-Ala studied in DMSO.[5] In such an orientation, the V6 methyl group contributes to the formation of the hydrophobic binding pocket, which is formed between ring 2 and the ring 6 chlorine substituent.[5] In the other conformation, the vancosamine lies on the back of the molecule (Figure 7B,D) with the methyl groups directed away from the binding cleft. The two orientations of the sugar substituent are similar to those in the crystal structure of an asymmetric vancomycin dimer which has recently appeared.[28]

The existence of two main conformations which differ by a rotation of the ring 4 acylglucosamine substituent was also observed for the gylcopeptide antibiotic teicoplanin.[29] In one conformation, the hydrophobic face of the glucose ring lies over the binding pocket and is proposed to increase the binding through the hydrophobic effect. In contrast to vancomycin, the two orientations of the sugar substituent for teicoplanin are observed for the free and bound forms.

Minor differences in the ϕ_3 and ϕ_4 dihedral angles between the two conformations of vancomycin confirm the flexibility of the backbone dihedral angles as observed from the DG calculations. Moreover, the violation of the w3−x2 NOE in all vancomycin structures indicates that the two preferred conformations are not sufficient to fulfill all of the experimental observations. Including a third conformation with w3 projecting away from the carboxylate of the binding pocket, as is observed for aglyco-vancomycin (discussed below), allows for the fulfillment of this NOE. The presence of this third conformation, the so-called β-pleated sheet form of residues 2, 3, and 4, has been predicted for vancomycin in DMSO.[30] These authors proposed conformational flexibility in this portion of the molecule based on the observation of mutually exclusive NOEs and broad resonances of w2, w3, and w4 amide protons.

The two conformations of vancomycin also differ in the region of residues 5 and 7 with the covalently linked aromatic rings, which form the wall in the binding pocket and are thought to turn the ligand toward the

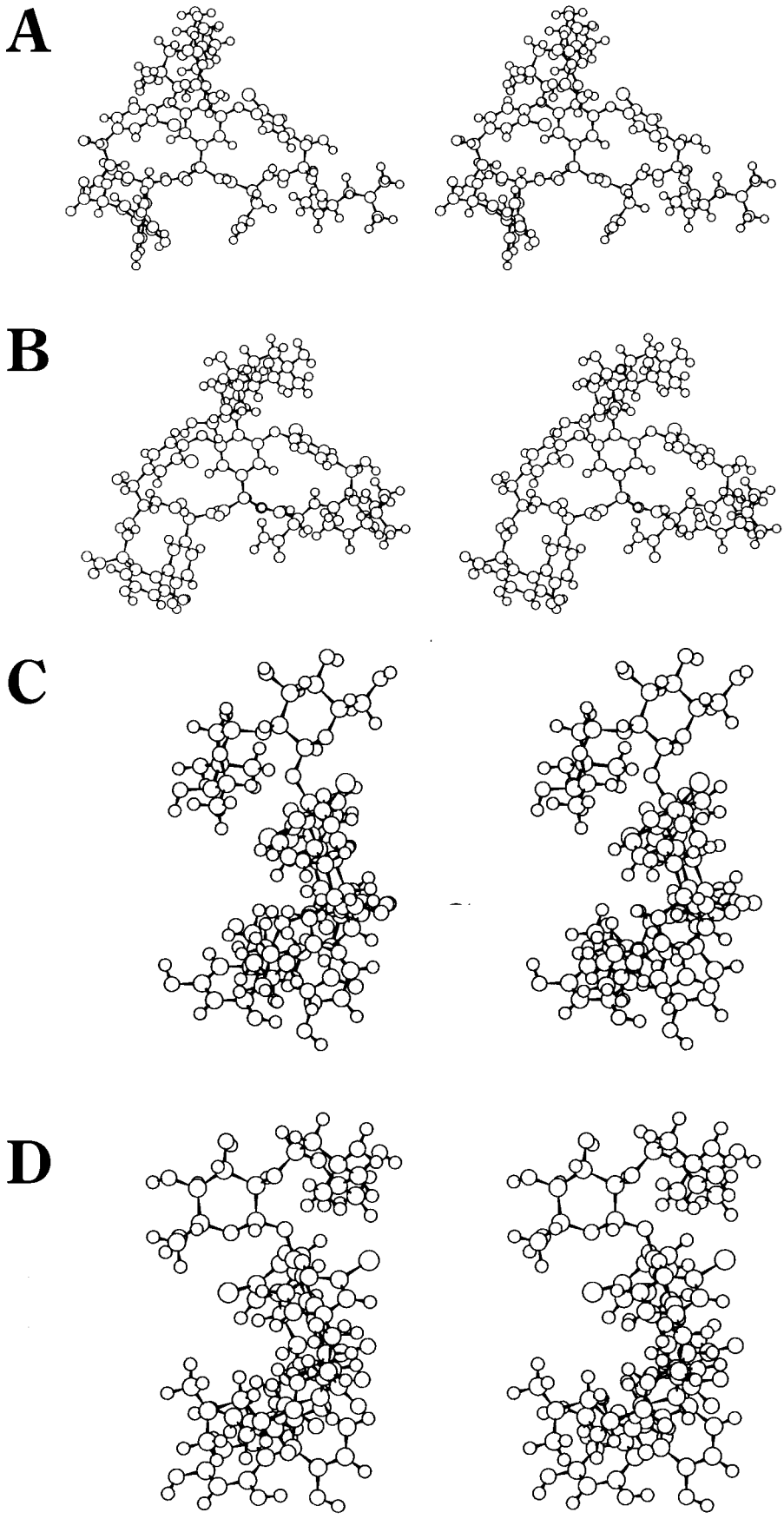

Figure 7. Stereoview of the two conformations of vancomycin observed in DMSO: V6 methyl group in front, front view (panel A), side view (panel C); V6 methyl on the rare side, front view (panel B), side view (panel D). Both conformers are present in solution, and only by considering both can all of the NOEs be fulfilled.

Table 2. Average Dihedral Angles (deg) from the NOE-Restrained MD Simulations of Aglyco-vancomycin and Vancomycin[a]

		vancomycin sugar at position 1			vancomycin sugar at position 2		
torsion	aglyco-vancomycin	1	2	3	1	2	3
residue 2							
ϕ	−177	70	68	120	73	75	119
ψ	−150	69	66	75	71	68	73
nw2−cx2−cz2−c2a	−172	−85	−88	−85	−88	−86	−84
cx2−cz2−c2a−c2b	−98	−124	−117	−123	−123	−118	−119
residue 3							
ϕ	−171	−123	−130	−126	−115	−126	−123
ψ	−116	−107	−106	−114	−110	−106	−106
residue 4							
ϕ	109	151	150	146	123	129	121
ψ	−148	−126	−128	−129	−133	−135	−136
residue 5							
ϕ	146	146	148	143	149	144	146
ψ	−143	−153	−150	−154	−141	−147	−146
nw5−cx5−c5a−c5b	126	121	122	120	132	128	128
residue 6							
ϕ	−99	−98	−98	−100	−98	−99	−100
ψ	134	142	141	140	136	140	138
nw6−cx6−cz6−c6a	−61	−68	−67	−66	−62	−61	−62
cx6−cz6−c6a−c6b	−78	−65	−66	−67	−76	−75	−76
residue 7							
ϕ	−73	−93	−90	−98	−81	−82	−81
nw7−cx7−c7a−c7b	−86	−70	−75	−54	−87	−82	−84
interresidue							
c2c−c2d−o2d−c4c	98	75	78	71	81	88	79
c2d−o2d−c4c−c4b	−11	31	23	32	4	−7	2
c4d−c4e−o6d−c6d	170	−132	−132	−138	−175	−164	−174
c6c−c6d−o6d−c4e	81	48	49	52	74	69	74
c5b−c5c−c7b−c7c	−109	−104	−108	−103	−111	−108	−108
c4c−c4d−og1−cg1		136	135	134	−62	−60	−67
c4d−og1−cg1−cg2		−168	−168	−167	−172	−178	−175
cg1−cg2−ov1−cv1		139	140	136	139	139	138
cg2−ov1−cv1−cv2		−172	−171	−172	−171	−172	−171

[a] The numbers 1, 2, and 3 denote different starting structures chosen from the families of DG structures of vancomycin (run with two different orientations of the disaccharide substituent).

disaccharide region when forming the complex with the antibiotic dimer.[8] There are small variations of the ϕ_7 and nw7−cx7−c7a−c7b dihedral angles between the two families. There is a slight change in the orientation of the w7 proton forming the hydrogen bond with the carbonyl of the second D-Ala residue upon binding to the cell-wall precursor. This amide is pointing toward the binding pocket in all conformations. There are also differences in the orientation of the ring composed of residues 5, 6, and 7 relative to the core ring, which is almost perpendicular in the conformation with the V6 methyl group in front of the molecule and more parallel in the other (an orientation similar to that was observed for aglyco-vancomycin).

The effect of the vancosamine position on the vancomycin rigid framework is illustrated in Figure 8. The molecules are viewed from the top of the aglycon, edge on with aromatic ring 4 (the sugar substituent removed for clarity). The conformations differ in the orientation of the antibiotic backbone, which affects the position of atoms forming the hydrophobic pocket of the molecule. These changes are expressed in differences of the c2c−c2d−o2d−c4c, c2d−o2d−c4c−c4b, c4d−c4e−o6d−c6d, and c6c−c6d−o6d−c4e dihedral angles (see Table 2). In the conformation with the vancosamine oriented above the binding pocket, the peptide backbone projects at an angle of approximately −30° from ring 4 (Figure 8A). In the conformer with the sugar on the other side, the peptide backbone aligns almost perfectly with ring 4 (Figure 8B). In contrast, the conformation of aglyco-vancomycin has the peptide backbone projecting at an angle of approximately 30° (Figure 8C).

The different alignment of the side chain of Asn-3 observed between vancomycin and aglyco-vancomycin is in complete agreement with the different NOEs for this residue (Figure 3). In aglyco-vancomycin, the side chain is closer to ring 2 and lies above the plane of the backbone (Figure 9). In both conformational families of vancomycin, the side chain lies below the plane of the backbone. The participation of the side chain of Asn-3 in intramolecular hydrogen bonds is not significant: the hydrogen bond between the carbonyl and the w4 amide proton was observed in only three of the MD simulations and then for only 25% or less of the MD production period. The Asn-3 side chain was found to be biologically important,[31] and participation of the side chain amide in the hydrogen-bonding network for the recognition of the carboxylate of the cell-wall precursor has been identified.[8] On the other hand, in the crystal structure of the vancomycin dimer/acetate complex, only the intramolecular hydrogen-bonding interaction between the Asn-3 side chain and the w3 and w4 amide protons was observed.[28] All MD structures have an Asn-3 χ_1 of 180°. However, the fact that no NOE between the hw4 and $h3a^S$ is observed indicates that the other rotamers are probably populated as well. The extraction of coupling constants which would help define the conformation of the side chain resulted in very inaccurate values because of broad resonances of the corresponding protons.

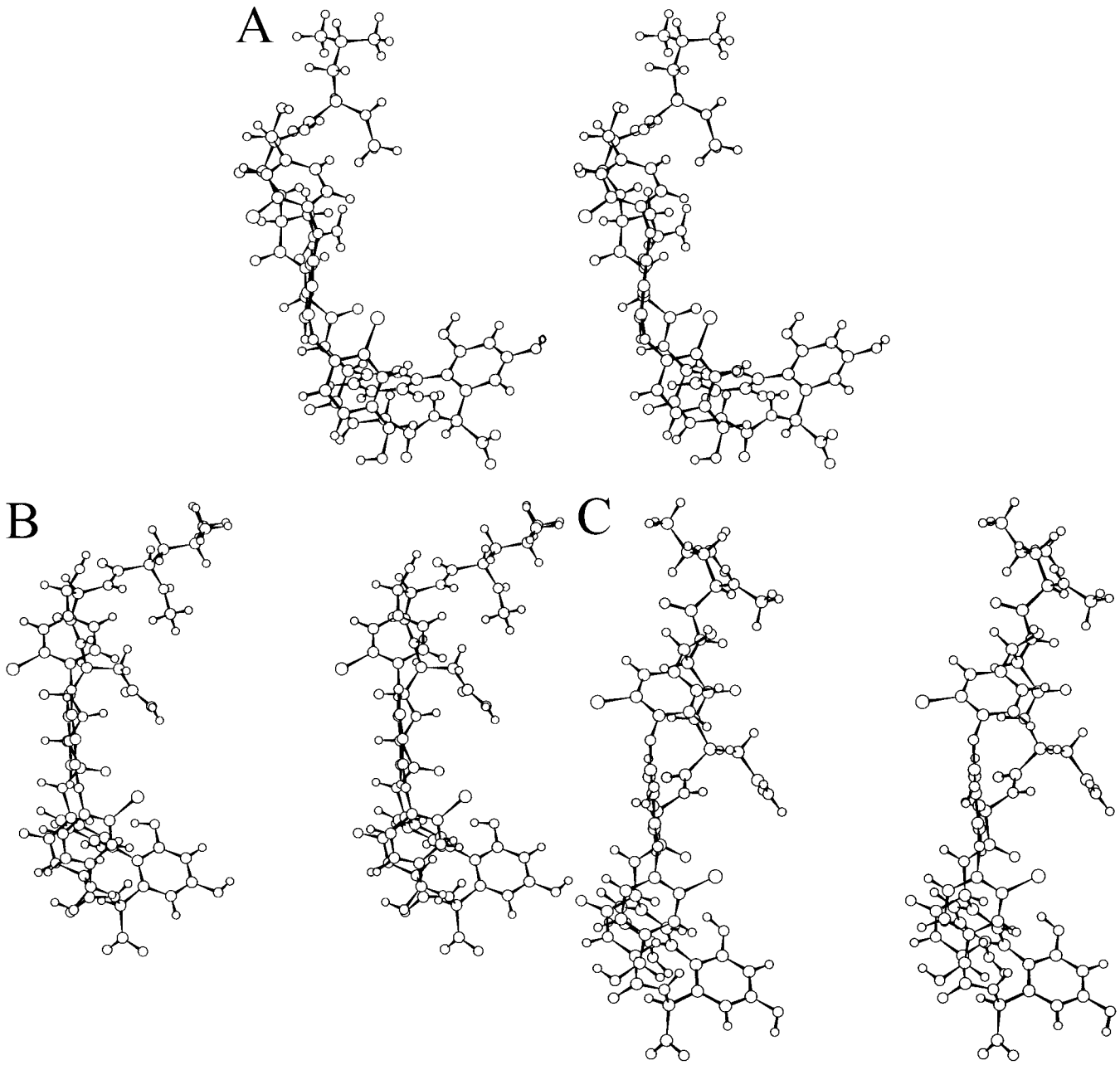

Figure 8. Illustration of the conformational differences of the central aromatic ring, ring 4, with respect to the peptide backbone: (A) vancomycin with V6 methyl group in front, (B) vancomycin with V6 methyl group on the rare side, and (C) aglyco-vancomycin. The view is from the top of the aglycon, looking edge on to ring 4. The peptide backbone is oriented at approximately −30° in A, is almost parallel in B, and approximately 30° for aglyco-vancomycin (C).

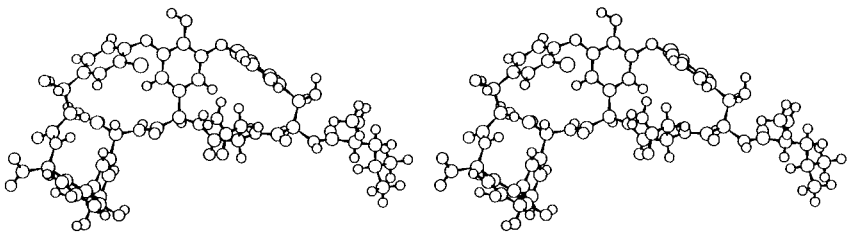

Figure 9. Stereoview of the conformation of aglyco-vancomycin observed in DMSO. The orientation is the same as that used for the two conformations of vancomycin depicted in Figure 7.

Another difference in the conformations of vancomycin and aglyco-vancomycin concerns the hydrogen-bonding network in the binding to the cell-wall precursor and formation of the antibiotic dimer. As illustrated in Figure 8 there is a different alignment of the w3 amide, which forms hydrogen bonds with the carboxylate of the cell-wall precursor. In the conformation of aglyco-vancomycin, the w3 amide is pointing in an unfavorable direction for the formation of this hydrogen bond. There are also variations in the alignment of the other two amide protons, w2 and w4, and the c3 carbonyl, which participate in intermolecular hydrogen-

bonding. This carbonyl forms a hydrogen bond with the w6 amide of another molecule in the antibiotic dimer.

Conclusions

The effect of the sugar substituent in the formation of antibiotic dimers and in the complexation with cell-wall peptides has been extensively studied.[5,13,16,32] The sugar substituent greatly enhances the dimerization of the antibiotic, which coupled with the cooperative effect between dimerization and cell-wall binding[14] indicates a pharmacologically important role for the glycosylation of the antibiotics. The observed reduction in cell-wall binding upon the removal of the amino sugar has been attributed to the V6 methyl group which contributes to the hydrophobic binding pocket of vancomycin.[5,30]

Our results indicate that the disaccharide substituent leads to significant conformational changes of the antibiotic aglycon. The sugars affect the orientation of the aromatic rings with respect to the antibiotic backbone and influence the alignment of the amide protons important for dimerization and cell-wall binding. Another important effect is the introduction of mobility in the antibiotic aglycon. Two conformational families of vancomycin, differing in the positioning of the vancosamine substituent, were observed. In contrast, only one preferred conformation was observed for aglycovancomycin. It seems that the sugar substituent introduces mobility into the rigid framework of the antibiotic by a dynamic process of switching positions between the front and back sides of the molecule. This may be important in the molecular recognition process and enable the appropriate conformational changes required for the antibiotic to bind to the cell-wall. The alignment of the amide protons in the conformation of aglyco-vancomycin is unfavorable for complexation with the cell-wall precursor; this could be another factor leading to the reduced biological activity of the aglycovancomycin in comparison to vancomycin.

While this manuscript was in preparation, the crystal structure of an asymmetric vancomycin dimer was published.[28] In contrast to our results, the core of the molecule was observed to be structurally rigid. However, the crystal-packing forces and the interaction between the two monomers, as well as the interaction between the sugar substituents in the dimer, can reduce the mobility of the molecule. The structures of vancomycin from the study here and in the crystal are similar, particularly with regard to the two possible orientations of the sugar, alignment of the peptide backbone, and position of the side chain of Asn-3. The major difference is the relative orientation of the macrocyclic ring composed of residues 5, 6, and 7. In the crystal, this macrocycle is more parallel relative to the core ring, in contrast to a more orthogonal orientation in solution. Another difference between the X-ray and solution structures is the asymmetry of the monomers within the molecular dimer: the average pairwise rmsd of the 50 atoms of the three macrocyclic rings composed of residues 2−3−4, 4−5−6, and 5−6−7 for the two monomers in the X-ray structure is 0.18 Å, while a value of 0.8 Å is observed in solution. The asymmetry in solution is therefore slightly greater than that observed in the solid state.

Materials and Methods

Nuclear Magnetic Resonance. NMR spectra were recorded on Varian INOVA 600-MHz and Bruker DPX 300-MHz spectrometers in DMSO-d_6 at 298 K. The sample concentrations were 2 mM. The DQF-COSY[33] and ^{1}H−^{13}C HSQC[34,35] experiments were performed with gradients. The TOCSY[36,37] and NOESY[38] experiments were recorded using standard pulse sequences in the phase-sensitive mode. The TOCSY spectra were recorded with an MLEV-17[37] mixing sequence of 60 ms and a 10-kHz spin−lock field strength. NOESY spectra were measured at six different mixing times (50, 100, 150, 200, and 250 ms) for vancomycin and two (50 and 150 ms) for the aglycovancomycin. The ^{1}H sweep width was 6662 at 600 MHz. Typically, the homonuclear proton spectra were acquired with 4096 data points in t_2, 16−64 scans, 256−512 complex points in t_1, and a relaxation delay of 1−1.5 s. The ^{1}H−^{13}C HSQC spectra were recorded with 2048 data points in t_2, 64 scans per increment, 128 complex points in t_1, and a relaxation delay of 1 s. The ^{13}C spectral width was 23 795 Hz at 600 MHz. Data were processed and analyzed with FELIX software package from Biosym Technologies. Spectra were zero-filled two times and apodizied with a squared sine bell function shifted by $\pi/2$ in both dimensions. Distances were calculated from cross-peak volumes in NOESY spectra by the routine within the FELIX program. The pseudoatom correction was added for the methyl groups, and the ±10% was applied to the distance, to produce the upper and lower limit constraints.

Distance Geometry. DG calculations were carried out using a home-written program based on the random metrization algorithm;[18] 100 structures were generated by choosing the distances randomly between upper and lower bound constraints determined from holonomic and experimental NOE constraints. The structures were first embedded in four dimensions and then partially minimized by conjugate gradient minimization. The structures were further refined by distance-driven dynamics (DDD)[39] beginning at 500 K for 100 ps and then with a gradual reduction in temperature over the next 50 ps. The holonomic and experimental distance constraints and a chiral penalty function were used for the generation of violation energy and forces in the DDD procedure. Three-dimensional coordinates were created by the EMBED algorithm[40] and then the optimization and DDD procedures repeated. The floating chirality DG calculations[24] were carried out by removal of the chiral constraint on the asparagine side chain so that the methylene protons were free to switch prochiral positions. The ensemble calculations were identical with those for the DDD method, except that the penalty expression for the experimental restraints and the forces are generated from an ensemble average.[19,20,41]

Molecular Dynamics. MD simulations were performed with DISCOVER (consistent valence force field) and INSIGHT II from Biosym Technologies. Several simulations with different starting structures for both antibiotics, picked from the families of DG structures, were carried out in DMSO.[21] The molecule with all atoms treated explicitly was centered in a cubic box ($x = y = z = 40$ Å) using three-dimensional periodic boundary conditions. The dielectric constant was set to 1.0. Neighbor lists for calculation of nonbonded interactions were updated every 10 fs within a radius of 14 Å. The actual calculation of nonbonded interactions was carried out up to a radius of 12 Å without use of switching functions. A time step of 1 fs was employed for the MD simulation. The simulation protocol consisted of two minimization cycles (steepest descent and conjugate gradients), first with the solute fixed and then with all the atoms allowed to move freely. The convergence criterion was 1 kcal Å^{-1}. The initial MD phase of the calculation involved a gradual heating, starting from 100 K and then increasing to 150, 200, 250, and finally 300 K in steps of 0.5, 0.5, 5, 1, and 5 ps, respectively, each by direct scaling of the velocities. The NMR-derived distance restraints with a force constant of 10 kcal mol^{-1} Å^{-1} were applied during the complete simulation. Configurations were saved every 1 ps for another 200 ps of dynamics. The last 100 ps of the

trajectory was used for analysis of NOE distance violations and dihedral angles.

Acknowledgment. We gratefully acknowledge financial support from the Ministry of Science and Technology of Slovenia (Grant S17860-0104-96 awarded to S.G.G.). This work was supported, in part, by NIH Grant R29-GM54082 (awarded to D.F.M.). We also wish to thank Dr. Darko Kocjan of LEK Pharmaceuticals for providing the samples of vancomycin and aglyco-vancomycin.

References

(1) Courvalin, P. The resistance of *enterococci* to glycopeptides. *Antimicrob. Agents Chemother.* **1990**, *34*, 2291−2296.
(2) Hakenbeck, R. In *Bacterial Cell Wall*; Ghuysen, J.-M., Hakenbeck, R., Eds.; Elsevier: New York, 1994; pp 535−546.
(3) Neu, H. C. The crisis in antibiotic resistance. *Science* **1992**, *257*, 1064−1073.
(4) Fesik, S. W.; O'Donnel, T. J.; Gampe, R. T.; Olejniczak, E. T. Determining the structure of a glycopeptide-Ac_2-Lys-D-Ala-D-Ala complex using NMR parameters and molecular modeling. *J. Am. Chem. Soc.* **1986**, *108*, 3165−3170.
(5) Kannan, R.; Harris, C. M.; Harris, T. M.; Waltho, J. P.; Skelton, N. J.; Williams, D. H. Function of the amino sugar and N-terminal amino acid of the antibiotic vancomycin and its complexation with cell-wall peptides. *J. Am. Chem. Soc.* **1988**, *110*, 2946−2953.
(6) Waltho, J. P.; Williams, D. H.; Stone, D. J. H.; Skelton, N. J. Intramolecular determination of conformation and mobility within the antibiotic vancomycin. *J. Am. Chem. Soc.* **1988**, *110*, 5638−5643.
(7) Molinari, H.; Pastore, A.; Lian, L.; Hawkes, G. E.; Sales, K. Structure of vancomycin and a vancomycin/D-Ala-D-Ala complex in solution. *Biochemistry* **1990**, *29*, 2271−2277.
(8) Prowse, W. G.; Kline, A. D.; Skelton, A.; Loncharich, R. J. Conformation of A82846B, a glycopeptide antibiotic, complexed with its cell-wall fragment: an asymmetric homodimer determined using NMR spectroscopy. *Biochemistry* **1995**, *34*, 9632−9644.
(9) Wright, G. D.; Walsh, C. T. D-alanyl-d-alanine ligases and the molecular mechanism of vancomycin resistance. *Acc. Chem. Res.* **1992**, *25*, 468−473.
(10) Bugg, T. D. H.; Wright, G. D.; Dutka-Malen, S.; Arthur, M.; Courvalin, P.; Walsh, C. T. Molecular basis for vancomycin resistance in *Enterococcus faecium* BM4147 − biosynthesis of a depsipeptide peptidoglycan precursor by vancomycin resistance proteins Van H and Van A. *Biochemistry* **1991**, *30*, 10408−10415.
(11) Messer, J.; Reynolds, P. E. Modified peptidogylcan precursor produced by glycopeptide-resistant *enetrococci*. *FEMS Microbiol. Lett.* **1992**, *94*, 195−200.
(12) Arthur, M.; Courvalin, P. Genetics and mechanism of glycopeptide resistance in *enterococci*. *Antimicrob. Agents Chemother.* **1993**, *37*, 1563−1571.
(13) Mackay, J. P.; Gerhard, U.; Beauregard, D. A.; Maplestone, R. A.; Williams, D. H. Dissection of the contributions toward dimerization of glycopeptide antibiotics. *J. Am. Chem. Soc.* **1994**, *116*, 4573−4580.
(14) Mackay, J. P.; Gerhard, U.; Beauregard, D. A.; Westwell, M. S.; Searle, M. S.; Williams, D. H. Glycopeptide antibiotic activity and the possible role of dimerization: A model for biological signaling. *J. Am. Chem. Soc.* **1994**, *116*, 4581−4590.
(15) Beauregard, D. A.; Williams, D. H.; Gwynn, M. N.; Knowles, D. J. C. Dimerization and membrane anchors in extracellular targeting of vancomycin group antibiotics. *Antimicrob. Agents Chemother.* **1995**, *39*, 781−785.
(16) Groves, P.; Searle, M. S.; Mackay, J. P.; Williams, D. H. The structure of an asymmetric dimer relevant to the mode of action of the glycopeptide antibiotics. *Structure* **1994**, *2*, 747−754.
(17) Nagarajan, R. J. Structure−activity relationship of vancomycin-type glycopeptide antibiotics. *J. Antibiot.* **1993**, *46*, 1181−1195.
(18) Havel, T. F. An evaluation of computational strategies for use in the determination of protein structure from distance constraints obtained by nuclear magnetic resonance. *Prog. Biophys. Mol. Biol.* **1991**, *56*, 43−78.
(19) Mierke, D. F.; Scheek, R. M.; Kessler, H. Coupling constant restraints in ensemble calculations. *Biopolymers* **1994**, *34*, 559−563.
(20) Mierke, D. F.; Kurz, M.; Kessler, H. Peptide flexibility and calculation of an ensemble of molecules. *J. Am. Chem. Soc.* **1994**, *116*, 1042−1049.
(21) Mierke, D. F.; Kessler, H. Molecular dynamics with dimethyl sulfoxide as a solvent. Conformation of a cyclic hexapeptide *J. Am. Chem. Soc.* **1991**, *113*, 9466−9470.
(22) Harris, C. M.; Kopecka, H.; Harris, T. M. Vancomycin: Structure and transformation to CDP-I. *J. Am. Chem. Soc.* **1983**, *105*, 6915−6922.
(23) Pearce, M. C.; Williams, D. H. Complete assignment of the ^{13}C NMR spectrum of vancomycin. *J. Chem. Soc., Perkin Trans.* **1995**, *2*, 153−157.
(24) Weber, P. L.; Morrison, R.; Hare, D. Determining stereospecific ^1H nuclear magnetic resonance assignments from distance geometry calculations. *J. Mol. Biol.* **1988**, *204*, 483−487.
(25) Neuhaus, D.; Williamson, M. *The Nuclear Overhauser Effect in Structural and Conformational Analysis*; VCH Publishers: New York, 1988; p 446.
(26) Havel, T. F. The sampling properties of some distance geometry algorithms applied to unconstrained polypeptide chains: a study of 1830 independently calculated conformations. *Biopolymers* **1990**, *29*, 1565−1585.
(27) Sheldrick, G. M.; Jones, P. G.; Kennard, O.; Williams, D. H.; Smith, G. A. Structure of vancomycin and its complex with acetyl-D-alanyl-D-alanine. *Nature* **1992**, *271*, 223−225.
(28) Loll, P. J.; Bevivino, A. E.; Korty, B. D.; Axelsen, P. H. Simultaneous recognition of a carboxylate-containing ligand and an intramolecular surrogate ligand in the crystal structure of an asymmetric vancomycin dimer. *J. Am. Chem. Soc.* **1997**, *119*, 1516−1522.
(29) Westwell, M. S.; Gerhard, U.; Williams, D. H. Two conformers of the glycopeptide antibiotic teicoplanin with distinct ligand binding sites. *J. Antibiot.* **1994**, *48*, 1292−1298.
(30) Williams, D. H.; Waltho, J. P. Molecular basis of the activity of antibiotics of the vancomycin group. *Biochem. Pharmacol.* **1988**, *37*, 133−141.
(31) Nagarajan, R. J. *Glycopeptide Antibiotics*; Marcel Dekker: New York, 1993.
(32) Gerhard, U.; Mackay, J. P.; Maplestone, R. A.; Williams, D. H. The role of the sugar and chlorine substituents in the dimerization of vancomycin antibiotics. *J. Am. Chem. Soc.* **1993**, *115*, 232−237.
(33) Rance, M.; Sorensen, O. W.; Bodenhausen, G.; Wagner, G.; Ernst, R. R.; Wütrich, K. Improved spectral resolution in COSY proton NMR spectra of proteins via double quantum filtering. *Biochem. Biophys. Res. Commun.* **1983**, *117*, 479−485.
(34) Bodenhausen, G.; Ruben, D. J. Natural abundance nitrogen-15 NMR by enhanced heteronuclear spectroscopy. *Chem. Phys. Lett.* **1980**, *69*, 185−189.
(35) Willker, W.; Leibfritz, D.; Kerssebaum, R.; Bermel, W. Gradient selection in inverse heteronuclear spectroscopy. *Magn. Reson. Chem.* **1993**, *31*, 287−292.
(36) Braunschweiler, L.; Ernst, R. R. Coherence transfer by isotropic mixing: application to proton correlation spectroscopy. *J. Magn. Reson.* **1983**, *53*, 521−528.
(37) Bax, A.; Davis, D. G. MLEV-17-based two-dimensional homonuclear magnetization transfer spectroscopy. *J. Magn. Reson.* **1985**, *65*, 355−360.
(38) Jeener, J.; Meier, B. H.; Bachmann, P.; Ernst, R. R. Investigation of exchange processes by two-dimensional NMR spectroscopy. *J. Chem. Phys.* **1979**, *71*, 4546−4553.
(39) Kaptein, R.; Boelens, R.; Scheek, R. M.; van Gunsteren, W. F. Protein structures from NMR. *Biochemistry* **1988**, *27*, 5389−5395.
(40) Crippen, G. M.; Havel, T. F. *Distance Geometry and Molecular Conformation*; Research Studies Press Ltd.: Somerset, England, 1988.
(41) Scheek, R. M.; Torda, A. E.; Kenmink, J.; van Gunsteren, W. F. *Computational Aspects of the Study of Biological Macromolecules by Nuclear Magnetic Resonance*; Plenum Press: New York, 1991; pp 209−217.

JM9705972